Hindawi Publishing Corporation
Mathematical Problems in Engineering
Volume 2013, Article ID 732325, 14 pages
http://dx.doi.org/10.1155/2013/732325

Research Article

Safety Monitoring Index of High Concrete Gravity Dam Based on Failure Mechanism of Instability

Shaowei Wang,[1,2,3] Chongshi Gu,[1,2,3] and Tengfei Bao[1,2,3]

[1] *State Key Laboratory of Hydrology-Water Resources and Hydraulic Engineering, Hohai University, Nanjing 210098, China*
[2] *National Engineering Research Center of Water Resources Efficient Utilization and Engineering Safety, Hohai University, Nanjing 210098, China*
[3] *College of Water-Conservancy and Hydropower, Hohai University, Nanjing 210098, China*

Correspondence should be addressed to Shaowei Wang; shaowei2006nanjing@163.com

Received 8 September 2013; Revised 14 November 2013; Accepted 14 November 2013

Academic Editor: Xiao-Wei Ye

Traditional methods of establishing dam safety monitoring index are mostly based on the observation data. According to the performance of dam-foundation system under the experienced loads, alarm values and extreme values are predicted for monitoring quantities. As for some dams, the potential most unfavorable loads may not yet have appeared, and dam bearing capacity may also decrease over time. Therefore, monitoring index determined by these methods can not reflect whether the dam will break or not. Based on the finite element method, to study the progressive instability failures of high concrete gravity dams under the failure modes of material strength degradation or uncertainty and extreme environmental loads during operation, methods of strength reduction and overloading are, respectively, used. Typical stages in the instability processes are identified by evaluation indicators of dam displacement, the connectivity of yield zones, and the yield volume ratio of dam concretes; then instability safety monitoring indexes are hierarchically determined according to these typical symptoms. At last, a case study is performed to give a more detailed introduction about the process of establishing safety monitoring index for high concrete gravity dams based on the failure mechanism of instability, and three grades of monitoring index related to different safety situations are established for this gravity dam.

1. Introduction

With the implementation of the National West to East Power Transmission Project, a large number of high dams are constructed or under construction in western China, in which concrete gravity dams are frequently adopted. The special mountain valleys in western China provide advantageous topographic conditions for the construction of high dams. However, dam safety becomes an important issue in the western area due to the complicated geological conditions as well as strong earthquakes of high frequency.

Structure safety monitoring is more frequently designed and implemented on civil engineering structures, such as dams, bridges, and high buildings. Meanwhile, analysis and back-analysis of the monitoring data are performed to evaluate the performance of these structures in time [1–5]. As for dams, dam failure is a progressive process, in which local damages accumulate firstly, then lead to the deterioration of dam safety situation, and finally cause the dam failure. Therefore, to avoid dam failure, it is necessary to monitor the dams and their foundations and timely detect and analyze dam abnormal symptoms according to the observation data [6]. To ensure the normal operation, monitoring quantity should not exceed its allowable value, namely, the safety monitoring index. Hence, monitoring index is defined as the extreme value of each monitoring quantities before dam failure, which is used to evaluate and monitor dam safety [7]. Before the nineteen sixties, engineers had not realized the importance of observation data in dam safety management so that further analyses were ignored, let alone the establishment of monitoring index and ternperatwre alarm, so dam safety monitoring system was not fully utilized. The failures of Malpasset arch dam and Vajont arch dam are both closely related to the absence of monitoring index [8]. The measured

displacement of Malpasset arch dam four mouths before its failure is significantly larger than the theoretical value, and the closer to dam bottom the more serious. Landslides on the left bank of Vajont arch dam began to creep slowly after the impoundment of upstream reservoir in 1960; the measured total displacement at the dam crest came up to 429 cm on October 7, 1963, and increased at an amazing speed of 48.3 mm/d during the last 12 days before failure. Ternperatwre alarms were not made for the occurrence of abnormities so that both dam failures occurred without any engineering or nonengineering measures, so the absence of monitoring index for Malpasset arch dam and Vajont arch dam restricted the function of their safety monitoring systems. The situation that monitoring quantity exceeds its monitoring index probably means the abnormity of dam safety, so it is a key problem for managers to determine the monitoring index scientifically.

As for gravity dams, dam failures are mainly caused by the instability of dam-foundation systems, and the failure process depends on failure modes [9, 10]. Due to the complexity and specificity of each dam-foundation system, failure mechanisms and failure processes are different from dam to dam even if under the same failure mode. Therefore, it is necessary to simulate the real failure process and study the failure mechanism of instability under different failure modes, and the instability safety monitoring index of high concrete gravity dams should be determined according to the typical symptoms in the simulated failure process.

This paper firstly makes a brief summary about the current theories and methods of establishing dam safety monitoring indexes, in which disadvantages of each method are analyzed. Then, based on the traditional finite element structural analysis method, considering the most probable potential failure modes of material degradation or uncertainty and extreme external environmental loads during dam operation, methods of strength reduction and overloading are, respectively, used in this paper to study the progressive instability failure process of high concrete gravity dams. Typical stages in the instability processes are identified by evaluation indicators of dam displacement, the connectivity of yield zones, and the yield volume ratio of dam concretes; then instability safety monitoring index of high concrete gravity dams is determined according to these typical symptoms. At last, the proposed method for establishing instability safety monitoring index of high concrete gravity dams is studied in detail with a practical engineering.

2. Research Situation of Dam Safety Monitoring Index

Current dam safety monitoring items are deformation, stress, uplift pressure, seepage, crack opening, and so on. Monitoring indexes for dam stress, uplift pressure, and seepage are determined according to the hydraulic specifications, and these items are often established for local areas where the monitoring quantities should be controlled strictly. Especially for dam stress, the stress-controllable areas, such as dam heel and dam toe, are also the stress concentration areas in the finite element method (FEM), so it is difficult to determine a reasonable stress control standard for these areas by FEM simulation [11]. As for the crack opening, it is not easy to determine the monitoring index by hydraulic specifications due to the complex opening mechanism of cracks. However, crack opening is the same as other monitoring items that only local damages may appear when its monitoring index is exceeded, and obvious abnormality will be directly reflected on dam deformation even if the rapid development of these local damages will result in the dam failure. Among all these monitoring items, deformation can directly reflect the global safety and the progressive failure process of dam-foundation system, so monitoring index for dam deformation is mostly determined as dam safety monitoring index [12].

The reasonable monitoring index can be used in analyzing and evaluating the situation of dam safety. However, due to the complexity of dam structures and the different material variation characteristics, comprehensive demonstration by different methods should be conducted to determine dam safety monitoring index. The mostly used methods for establishing the monitoring index at present are confidence interval method, typical low probability method, limit state method, and structural analysis method [13]. These methods are all without taking dam failure modes into consideration, let alone the instability mechanism and the progressive failure process under different failure modes. Therefore, advantages and disadvantages of these methods are analyzed before establishing the safety monitoring index of high concrete gravity dam based on failure mechanism of instability.

2.1. Confidence Interval Method. The basic principle of confidence interval method is the little probability event in statistics. According to the observation data, mathematical models (such as statistical model, hybrid model, and deterministic model) are established between monitoring effect quantities and environmental variables, and these models are used in calculating the deviations $(\hat{y} - y)$ between the calculated values $(\hat{y})$ and the measured values y of monitoring effect quantities in the domain of dam experienced loads. If the deviations are within the confidence band of $\Delta = \pm \beta\sigma$ with the probability of $1 - \alpha$ (α is the significance level, which is frequently determined as 1%~5%) and no obvious tendency variations are reflected on the monitoring effect quantities, then this dam is considered to be in normal condition. Therefore, dam monitoring index is established as follows:

$$\delta_m = \hat{y} + \Delta = \hat{y} \pm \beta\sigma, \tag{1}$$

where β is related to the significance level α and σ is the residual standard deviation of the mathematical model.

The frequently used confidence interval method and typical low probability method are both based on the observation data. According to the performance of dam-foundation system under the experienced loads, bearing capacities under the potential loads are evaluated, and the corresponding alarm values and extreme values are predicted for different monitoring effect quantities. However, dam safety information contained in the observation data varies from dam to dam due to the different experienced loads, especially for

some dams which have never experienced the potential most unfavorable loads [14]. Meanwhile, the bearing capacity of dam-foundation system is changing during dam operation. Therefore, monitoring index based on the observation data is without considering the real condition of dam safety, instead of really reflecting whether the dam will break or not, it only can be used as the warning index to identify the abnormality of monitoring quantities [15–17].

Based on the aforementioned analyses, disadvantages of the confidence interval method are as follows. (1) If the observation data under the most unfavorable load combination are absent, monitoring index based on the confidence interval method may be unreliable; it is just the alarming value for the experienced loads rather than the extreme values for dam failure. (2) The residual standard deviation σ of the mathematical model varies with the selected observation data sequences for the same monitoring points, and the significance level is determined with arbitrariness more or less. (3) Instead of associating with dam structural state and failure mechanism, the confidence interval method is totally dependent on statistical theories, so it is lack of physical concepts.

2.2. Typical Low Probability Method. The typical low probability method is the same as the confidence interval method that totally depends on the observation data; differences are that the former qualitatively associates with the controlling conditions of strength and stability by selecting the monitoring effect quantity (y_{mi}) or its component in mathematical models under the unfavorable load conditions (namely, the typical monitoring effect quantities). According to different dam types and the actual situation, y_{mi} is selected annually, and a random sample is constituted as $y = \{y_{m1}, y_{m2}, \ldots, y_{mn}\}$. Characteristics of the sample are described as follows:

$$\overline{y} = \frac{1}{n}\sum_{i=1}^{n} y_{mi}, \tag{2}$$

$$\sigma_E = \sqrt{\frac{1}{n-1}\left(\sum_{i=1}^{n} y_{mi}^2 - n\overline{y}^2\right)}. \tag{3}$$

The probability density function $f(y)$ (such as normal distribution, logarithmic normal distribution, and extreme-I distribution) of sample y is determined by statistical tests. Assuming that y_m ($y_{\max}$ or $y_{\min}$) is the extreme value of the monitoring quantity or its loading component, dam abnormality occurs if $y > y_{\max}$ or $y < y_{\min}$, and the probability is

$$P\left(y > y_{\max}\right) = P_a = \int_{y_{\max}}^{+\infty} f\left(y_{(\max)}\right) dy \quad \text{upper limit,} \tag{4}$$

or

$$P\left(y < y_{\min}\right) = P_a = \int_{-\infty}^{y_{\min}} f\left(y_{(\min)}\right) dy \quad \text{lower limit.} \tag{5}$$

Dam failure probability P_a is determined according to the importance of each dam. Then, dam safety monitoring indexes are established according to P_a and $f(y)$ ($f(y_{(\max)})$ or $f(y_{(\min)})$).

Monitoring indexes established by the typical low probability method can be determined as the extreme value of the whole dam operation period just on the condition that the dam has experienced all kinds of unfavorable conditions (including unfavorable load combinations and material degradation). Another problem is that the controlling conditions of strength and stability are only qualitatively associated, while quantitative analysis is ignored.

2.3. Limit State Method. It is assumed by the limit state method that each dam failure modes are corresponding to a certain load combination, and dam failures are mainly boiled down to the failure modes of strength, stability, cracks, and so on. The limit state equation is defined as follows:

$$Z = R - S \geq 0, \tag{6}$$

where R is the structure resistance, which is defined as material tension strength, compression strength, and shear strength for the evaluation of strength, and the antisliding force and fracture toughness for the evaluation of stability and cracking, respectively; S is the load effect, which is determined as extreme stress, sliding force, and stress intensity factor for the evaluation of strength, stability, and cracking, respectively.

The limit state method shows a relatively clear physical concept by quantificationally contacting with dam strength and stability. However, dam strength is based on the point failure criterion, which cannot reflect the global safety of dam-foundation system; as for dam stability, sliding surface should be assumed in advance for the overall sliding failure criterion, and the stability cannot be directly reflected by the monitoring quantities.

2.4. Traditional Structural Analysis Method. As for the traditional structural analysis method, it, respectively, connects the three safety states (normal, abnormal, and dangerous) in dam safety monitoring standard with three structural behaviors (linear elastic, elastic-plastic, and failure), and three levels of safety monitoring index are established as follows.

Monitoring index of grade one:

$$\delta_1 = F\left(\sigma_t < [\sigma_t],\ \sigma_c < [\sigma_c],\ K = \frac{R_{m1}}{S} \geq [K]\right). \tag{7}$$

Monitoring index of grade two:

$$\delta_2 = F\left(\sigma_t < \sigma_{tR},\ \sigma_c < \sigma_{cR},\ S \leq R_{m2},\ K_c \leq [K_c]\right). \tag{8}$$

Monitoring index of grade three:

$$\delta_3 = F\left(\sigma_t < \sigma_{tm}, \sigma_c < \sigma_{cm}, S \leq R_{m3}\right), \tag{9}$$

where σ_t and σ_c are tensile stress and compression stress of controlling areas; $[\sigma_t]$, σ_{tR}, and σ_{tm} are the allowable stress, yield strength, and ultimate strength of dam materials in the state of tension, respectively; $[\sigma_c]$, σ_{cR}, and σ_{cm} are the allowable stress, yield strength, and ultimate strength of

dam materials in the state of compression, respectively; S is the sliding force on the assumed sliding surface; K and $[K]$ are antislide stability safety coefficients of the actual value and the allowable value, respectively; R_{m1}, R_{m2}, and R_{m3} are antisliding forces, which are, respectively, calculated by material shear strength of sliding surface in states of proportion limit, yield limit, and the peak value; K_c and $[K_c]$ are stress intensity factor and fracture toughness, respectively.

It is the same as the limit state method that the aforementioned three levels of dam safety monitoring index are all based on the point failure criterion and the prior assumed sliding surface. However, due to the huge volume of dam body as well as the complicated geological condition in foundation, structural behaviors for each parts of the dam-foundation system are not the same. If fixed proportions of dam material in stages of linear elastic, elastic-plastic, and failure are used to decide the global structural behavior of dams, it is not easy to determine the proportions reasonably for different complex constructions. Therefore, it is unreasonable to determine the dam safety monitoring index based on the mechanical property of materials, and the failure mechanism of instability under different failure modes cannot be reflected by the traditional structural analysis method.

3. Simulation of the Progressive Failure of High Concrete Gravity Dam

The key problem of high concrete gravity dams is the stability. Practical experiences show that instability failure of gravity dams on rock foundation may occur in two modes [18]: (1) strength degradation caused by seepage, or some original weak structural surfaces, so dam failure occurs once the resistance force along some weak surfaces cannot stand up to the sliding force. Here, the sliding surfaces are usually the foundation plane, construction interfaces in dam body, and some weak structural surfaces in bedrocks. (2) Under the action of extreme environmental loads, pull broken areas and crushed areas in bedrocks of dam heel and dam toe are, respectively, performed, and dam failure of instability occurs accompanied with toppling. The construction interfaces in dam body can be avoided if dam concretes are poured in good quality, namely, the probability of instability failure in dam body is mostly decreased. As for the sliding along weak structural surfaces in bedrocks or the toppling-sliding failure, it mainly depends on the geological conditions. The special mountain valleys provide advantageous topographic conditions for the construction of high dams. However, these dams are often threatened by the complicated geological conditions as well as strong earthquakes of high frequency. Therefore, monitoring index for these high gravity dams must be determined according to the failure mechanism of instability under different potential failure modes.

Due to the complexity of bedrocks, sliding modes of gravity dams cannot be identified directly. Different combinations of foundation weak surfaces result in different sliding modes. According to the spatial distribution of foundation weak surfaces, sliding modes of gravity dams can be summarized into four types, which are single inclined plane sliding, double inclined plane sliding, crushed failure or bulged failure of the tail rock resistance block [19]. According to the dip angle of foundation weak surfaces, the aforementioned four modes can be summarized into two types, namely, the double or potential double inclined plane sliding and the translational sliding, which is shown in Figure 1. If the foundation weak structural surfaces, respectively, incline to the upstream and downstream directions and intersect at the bedrocks just below the foundation plane, the double inclined plane sliding occurs along the surface of ABC. As for the single inclined weak surface, such as the upstream direction inclined of B′C or the downstream direction inclined of AB″, failure areas of tension-shear or compression-shear may firstly appear at dam heel and dam toe, and the potential double inclined plane sliding occurs along the surface of AB′C and AB″C, respectively. The translational sliding occurs on the condition that the nearly horizontal gentle inclined weak structural surfaces are contained in bedrocks. Dam body and parts of bedrocks above the weak surface slide to the downstream integrally, and the tail rock resistance block tends to be crushed or bulged according to the buried depth of the weak surfaces and the mechanical property of upper rocks.

The stress field and displacement field of dam-foundation system can be calculated by FEM, and it is more reasonable to automaticly search the sliding surface according to dam deformation. On the other hand, methods of strength reduction and overloading can be, respectively, used to simulate material degradation or uncertainty and extreme external environmental loads during the service period. Hence, the FEM simulation is frequently used in studying the global safety of gravity dams [19, 20] and arch dams [21–23].

3.1. Overloading Method. To study the overloading capacity of gravity dam-foundation systems, overloading method is conducted under the assumption of unchangeable material properties of dam concretes and bedrocks. Under the normal load combination, external loads are increased until the dam failure by elevating the upstream water level or increasing the upstream reservoir water density, in which water density overloading method is commonly used by engineers. With the enlargement of upstream reservoir water density to K_p times (for normal load condition, the overloading parameter $K_p = 1$), stress field and displacement field are calculated by FEM, and the variation of dam safety is identified by the development of displacement and stress of typical points as well as the connectivity of plasticity yield zones of dam-foundation system. Hence, the overloading method can better simulate dam failures under the potential abnormal environmental loads, which are caused by overtopping, super earthquake, and the landslide of reservoir bank.

Taking a gravity dam section of unit width as an example, the dam height is 160 m and the widths at dam crest and bottom are 16 m and 125 m, respectively. The unit width dam section is designed with a vertical upstream dam surface and the downstream surface at a gradient of 1 : 0.75. According to the current Chinese specifications for seismic design of hydraulic structures DL5073-2000 [24], as for the traditional pseudo-static method, earthquake hydrodynamic pressure and inertial force are, respectively, calculated and

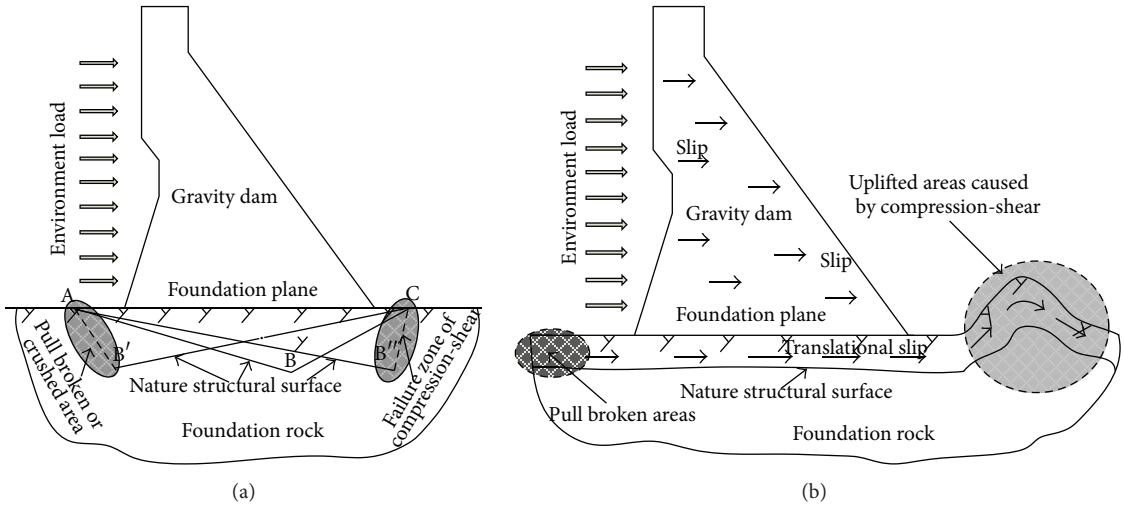

Figure 1: Sliding modes of gravity dam: (a) double or potential double inclined plane sliding; (b) translational sliding.

Table 1: The equivalent water density overloading parameter of earthquakes.

Peak acceleration of design earthquakes	0.1 g	0.2 g	0.4 g
Static water pressure of upstream (10^7 N)		11.6	
Earthquake hydrodynamic pressure (10^7 N)	0.38	0.76	1.51
Earthquake inertial force (10^7 N)	1.13	2.26	4.51
The total dynamic force/static water pressure	0.13	0.26	0.52
Overloading parameter of water density K_P	1.13	1.26	1.52

Notes: g is the gravitational acceleration, the normal water depth of upstream reservoir is 154 m.

shown in Table 1. It can be seen that the equivalent water density overloading parameter K_p comes up to 1.52 when the peak acceleration of earthquakes reaches 0.4 g. As for the actual situation, extreme external loads caused by strong earthquakes or landslides may be more serious than this, such as the failure of Vajont arch dam; later studies show that the huge water pressure caused by the landslide of reservoir bank is about 8 times of the designed loads.

3.2. Strength Reduction Method. Strength reduction method mainly considers the strength degradation during the service period and the uncertainty of material strength. Under the normal load combination, strengths of dam concretes and bedrocks are gradually reduced until the dam failure. Especially for bedrocks, due to the complexity of rock genesis and geotectonic movement, various faults, joints, and cracks are distributed complicatedly, so it is possible to make big differences of material properties in local small areas that cannot be systematically represented in the geological survey. Based on the Drucker-Prager yield criterion, the original shear strength parameters are denoted as c and f for cohesion and friction angle, respectively. Hence, the reduced parameters are denoted as c/K_s and f/K_s (for normal condition, the strength reduction parameter $K_s = 1$), and the gradually reduced shear strength is used by FEM simulation until the dam failure.

3.3. Comprehensive Method. Instead of the single action of overloading or strength degradation, dam failure is a progressive process from local damage to global failure under the comprehensive action of these two actors. The comprehensive method is the combination of overloading and strength reduction, so it seems more reasonable to simulate the dam failure. However, due to the specificity of dam projects, how to reasonably combine these two methods is still an unfathomed problem for engineers, and this situation limits the development of the comprehensive method in the studying of dam global safety.

3.4. Dam Safety Evaluation Indicators in the Progressive Failure

3.4.1. Dam Displacement. The global instability failure of gravity dams mainly resulted from the rapid development of infinite deformation caused by material strength degradation or abnormal environmental loads. No matter the sliding modes of inclined plane sliding or the translational sliding, dam displacements are all gradually increased before the dam failure. On the other hand, the progressive failure process of gravity dams under different failure modes can be simulated by FEM, and the theoretical displacements of typical stages in dam failure process can be determined as the instability safety monitoring indexes of gravity dams. The comparison of the observation displacement and its monitoring index shows the current situation of dam safety as well as the safety margin.

The simulation of dam failure by the geomechanical model test shows that when the parameters of strength reduction or overloading come up to a large amplitude, the rapidly increased nonlinear deformation results in the catastrophe of dam displacement, and the bearing capacity of dam-foundation system loses immediately. The development of dam displacement in the FEM simulation is similar to this,

so the catastrophe of dam displacement can be defined as the sign of losing bearing capacity for gravity dam-foundation systems, and the theoretical displacement at this moment is determined as the safety monitoring index of dam failure.

3.4.2. The Connectivity of Yield Zones. With the strength reduction or overloading, yield zones of dam-foundation system extend and join, and these yield zones are finally connected in dam body, along the foundation plane or in bedrocks. Here, yield zones are defined as the zones where the equivalent plastic strain is larger than a certain magnitude, and the equivalent plastic strain is defined as follows [25]:

$$\bar{\varepsilon}^p = \int \dot{\bar{\varepsilon}}^p dt = \int \left(\frac{2}{3} \dot{\varepsilon}_{ij}^p \dot{\varepsilon}_{ij}^p \right)^{1/2} dt, \tag{10}$$

where $\dot{\bar{\varepsilon}}^p$ is the equivalent plastic strain rate.

Plastic strain of tension, compression, and shear are all included in the equivalent plastic strain by integrating the equivalent plastic strain rate. Research results [21, 23] show that it is more suitable to set the amplitude of the total equivalent plastic strain at 10^{-4} to determine whether the concrete and bedrock are yielding or not.

Instead of the elastic-perfectly plastic material, both bedrock and dam concrete have the potential bearing capacity after yielding, so there is no obvious relationship between the connectivity of yield zones and the dam failure. Zheng et al. [26] pointed out that the connectivity of yield zones in soil is the necessary condition of soil sliding failure, not the sufficient condition, and the sign of soil sliding failure is identified as the rapid development of infinite deformation. Although the connectivity of yield zones does not immediately result in the dam failure, it still means the approach of ultimate bearing capacity. If engineering or nonengineering measures are not taken immediately to stop the deterioration of dam safety, dam deformation will increase sustainably and result in the dam failure at last.

3.4.3. The Yield Volume Ratio of Dam Body. Various disadvantageous weak structural surfaces are frequently distributed in dam foundation, and the working principle of gravity dams is that using the friction force caused by dam self-weight to resist the upstream horizontal water pressure to guarantee the stability. Meanwhile, yield zones of dam concretes mainly appeared at local areas of dam heel, dam toe, or the turning points of dam upstream and downstream surfaces. Therefore, if dam concretes are poured in good quality to ensure the designed strength and stiffness, global failure of gravity dams is unlikely to be caused by the yield of dam concretes. However, as for some high concrete dams which are constructed on the ideal bedrocks that the strength and stiffness are both guaranteed, dam concrete degradation or the abnormal environmental loads may result in a large proportion of yield concretes, and the rapidly increased infinite deformation of dam body determines the loss of bearing capacity of dam-foundation systems. For these high concrete gravity dams, catastrophe of the yield volume ratio of dam concretes can be determined as the sign of losing bearing capacity.

4. Determination of Instability Safety Monitoring Index of Gravity Dams

To establish the instability safety monitoring index for high concrete gravity dams, according to the actual conditions, such as the geological condition, environmental condition, and the degradation of dam concretes, it is necessary to firstly study the failure mechanism of instability under different potential failure modes. By simulating the progressive failures, typical stages in the instability failure process are identified by evaluation indicators of dam displacement, the connectivity of yield zones, and the yield volume ratio of dam concretes. Then, considering the condition that some of the failure conditions may not appear during dam operation, so these typical stages are analyzed and compared, and from the view of most unfavorable for dam safety, several typical stages are selected for hierarchically determining dam instability safety monitoring indexes. Finally, according to dam displacement fields at these typical stages, safety monitoring indexes are established for different dam safety grades. The flow chart of establishing safety monitoring index for high gravity dams based on the failure mechanism of instability is shown in Figure 2.

5. Case Study

A concrete gravity dam is located in the west of China, with a maximum dam height of 160.0 m, a crest elevation of 1424.0 m, and a crest axis length of 640.0 m. The highest dam section on the riverbed is selected to study the failure mechanism of instability and establish safety monitoring index. There are two nearly horizontal weak interlayers distributed in foundation bedrocks with the average buried depths of 30 m and 80 m, and the thicknesses of 1.65 m and 2.33 m, which are, respectively, denoted as $t1_b$ and $t1_a$. According to the boundaries of $t1_b$ and $t1_a$, foundation rocks are divided into three categories, which are, respectively, denoted as rock I, rock II, and rock III, from the ground surface to the deeper. The range of the FEM model is about two times of the maximum dam height in the upstream, downstream, and downward directions according to the dam heel and dam toe. Thicknesses of the weak interlayer in the FEM model are determined as the actual value. The gravity dam-foundation system is discretized into eight-node and six-node solid elements, with 15932 elements and 19056 nodes, in which the dam body contains 3549 elements and 4432 nodes. The FEM model is shown in Figure 3(a). Material parameters for dam body and its foundation are listed in Table 2.

To study the failure mechanism of instability by methods of strength reduction, overloading and the comprehensive method, evaluation indicators of dam displacement, the connectivity of yield zones, and the yield volume ratio of dam body are used to identify the safety variation of this high concrete gravity dam-foundation system in the progressive failure process. Five observation points of the plumb line in the monitoring system are determined as the typical points of dam displacement, and the elevations are 1424.0 m (dam crest) 1359.0 m, 1320.0 m, 1292.0 m, and 1264.0 m (foundation

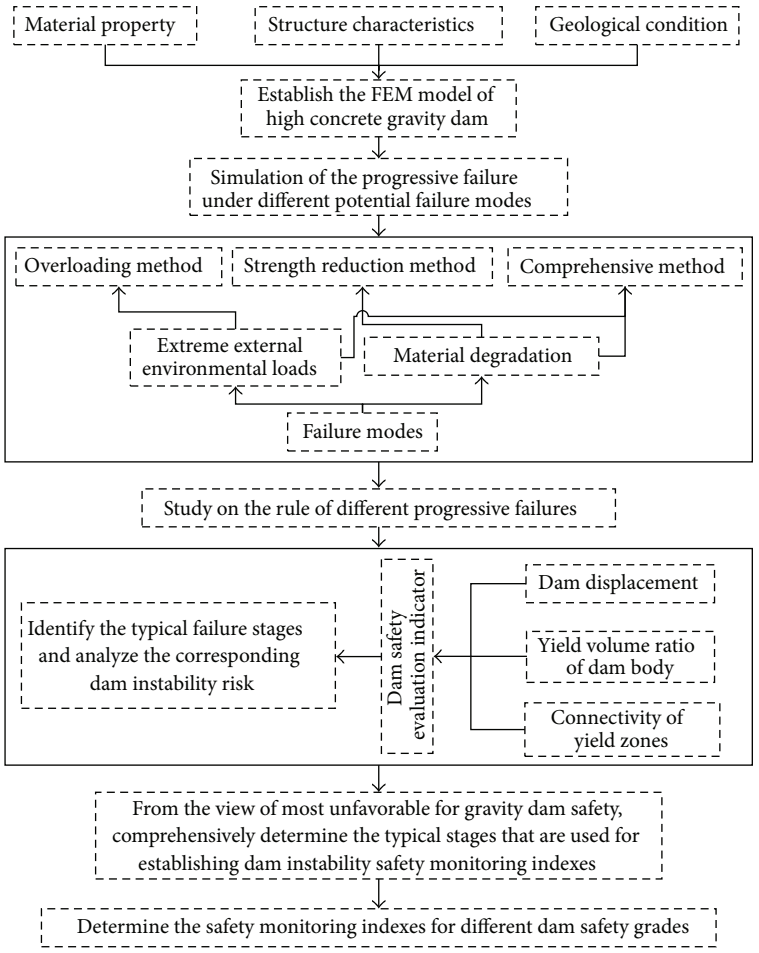

Figure 2: The flow chart of establishing safety monitoring index for high concrete gravity dams based on the failure mechanism of instability.

Table 2: Material parameters for dam body and its foundation.

	Elastic modulus E (GPa)	Poisson's ratio ν	Density ρ (kg/m^3)	Cohesion c (MPa)	Friction angle f
Dam body	25	0.167	2400	2.7	1.33
Rock I	4	0.27	2600	0.7	0.95
Rock II	8	0.27	2600	1.0	1.15
Rock III	10	0.27	2600	1.3	1.35
Weak interlayer	2	0.3	2500	0.4	0.73

plane), respectively. Distribution of the typical points is shown in Figure 3(b).

5.1. Material Model and Yield Criterion. Drucker-Prager yield criterion is commonly used for concretes and rocks as it can yield a smooth failure surface and is determined corresponding to the hydrostatic stress. Hence, the Drucker-Prager yield criterion is adopted in studying the failure mechanism of instability of high concrete gravity dams, which is presented as follows:

$$f = \alpha I_1 + \sqrt{J_2} - K = 0, \tag{11}$$

where I_1, J_2 are the first invariant of stress tensor and the second invariant of deviatoric stress tensor, respectively. α and K are parameters related to the material shear strength as follows:

$$\alpha = \frac{\sin\varphi}{\sqrt{3}\sqrt{3 + \sin^2\varphi}}, \tag{12}$$

$$K = \frac{3c\cos\varphi}{\sqrt{3}\sqrt{3 + \sin^2\varphi}}. \tag{13}$$

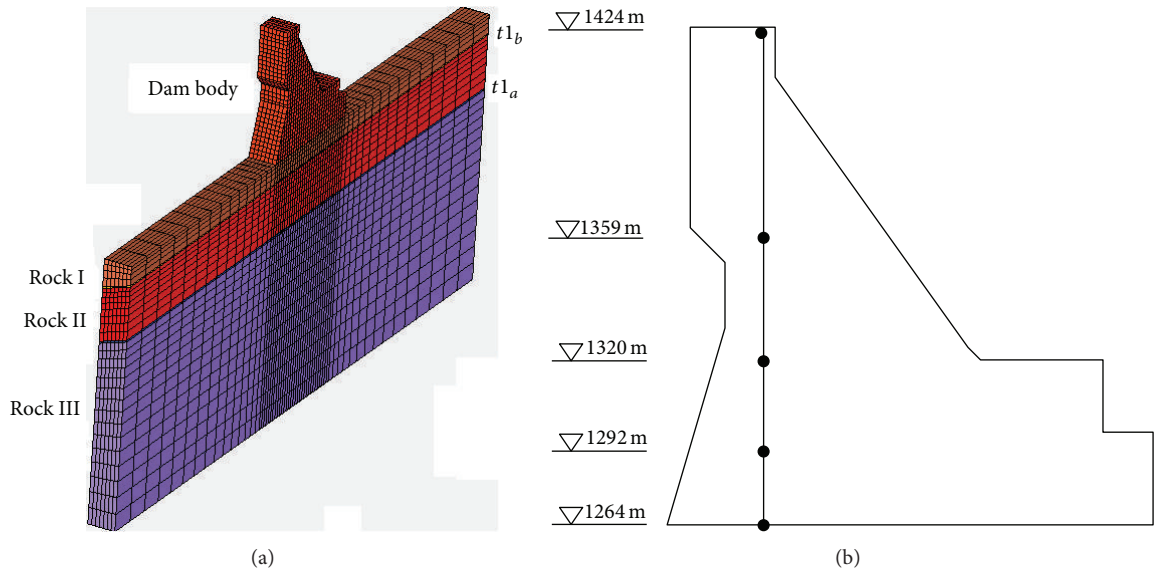

FIGURE 3: Integral FEM model and the typical points: (a) FEM model; (b) typical displacement points.

5.2. Simulation of the Progressive Failure under Different Failure Modes. Considering that the most probable potential failure modes are material degradation and extreme external environmental loads during the service period, hence, to establish dam safety monitoring index based on the risk of dam failure, methods of strength reduction and overloading are used in studying the failure mechanism of instability and the progressive failure process at first. Then, safety monitoring indexes are hierarchically determined according to the typical stages of the progressive failure and the actual dam situation.

5.2.1. Analysis Results of the Strength Reduction Method. The strength reduction method is used to simulate the material strength degradation and uncertainty. The constant load condition is the combination of upstream hydrostatic pressure (with the normal water level of 1418.0 m), dam self-weight, silt pressure, and uplift pressure. The elevation of silt sedimentation is 1335.0 m; the silt submerged unit weight and the friction angle are 12 kN/m^3 and 23°, respectively. The uplift pressure reduction coefficient of dam foundation impervious curtain is 0.25.

The progressive failure process of this gravity dam-foundation system under the simulation method of strength reduction is shown in Figure 4, in which the black zones are the failure regions where the total equivalent plastic strain is beyond the amplitude of 10^{-4}, and it has the same meaning in Figure 7.

Due to the existence of the stream direction horizontal weak interlayer, under the normal load condition, yield zones firstly appeared at the dam toe and its nearby bedrocks of the shallowly buried $t1_b$ interlayer. When the reduction parameter K_s reaches 1.2, the connectivity of yield zones is formed at the dam toe between the foundation plane and the $t1_b$ interlayer; namely, the potential downstream sliding surface is developed. With the continual increments of the reduction parameter, yield zones rapidly extend towards the upstream direction along the foundation plane and the $t1_b$ interlayer. When $K_s = 2.0$, the connectivity of yield zones from upstream to downstream is partly formed at the shallowly buried $t1_b$ interlayer on the right side of this dam section, and when $K_s = 2.2$, this yield zones are totally connected between the foundation plane and the $t1_b$ interlayer from dam heel to dam toe. Therefore, one of the potential sliding modes of this gravity dam is the translational sliding with three sliding surfaces, which are composed of the tension-shear crack zones at the dam heel, the $t1_b$ interlayer, and the compression-shear crushed zones at the dam toe. When $K_s = 3.0$, the connected yield zones extend to the $t1_a$ interlayer which is deeply buried with a depth of 80 m. Meanwhile, the strength reduction results in the connectivity of dam concretes between the dam heel and the turning point of the downstream dam surface. Thus, the connectivity of yield zones both appeared in dam body and foundation rocks, and the rapidly increased infinite deformation results in the catastrophe of dam displacement and the loss of bearing capacity at last.

The developments of dam displacement and dam body yield volume ratio with the strength reduction parameter are shown in Figures 5 and 6, and it is perfectly in accordance with the aforementioned progressive failure process. It can be seen from Figure 5 that when K_s is less than 2.2, the stream displacement of the selected five typical points remains largely unchanged, and yield zones rarely appeared in dam body. The relatively stable relationship between dam displacement and the reduction parameter indicates the unchanged stable status of this gravity dam. Then, dam concrete yields over a large area, while dam displacement slowly increases with a small amplitude. Reasons may be concluded as follows: the first one is that the connectivity of yield zones in dam body is not formed before K_s reaches 3.0. The other important reason is that the translational sliding

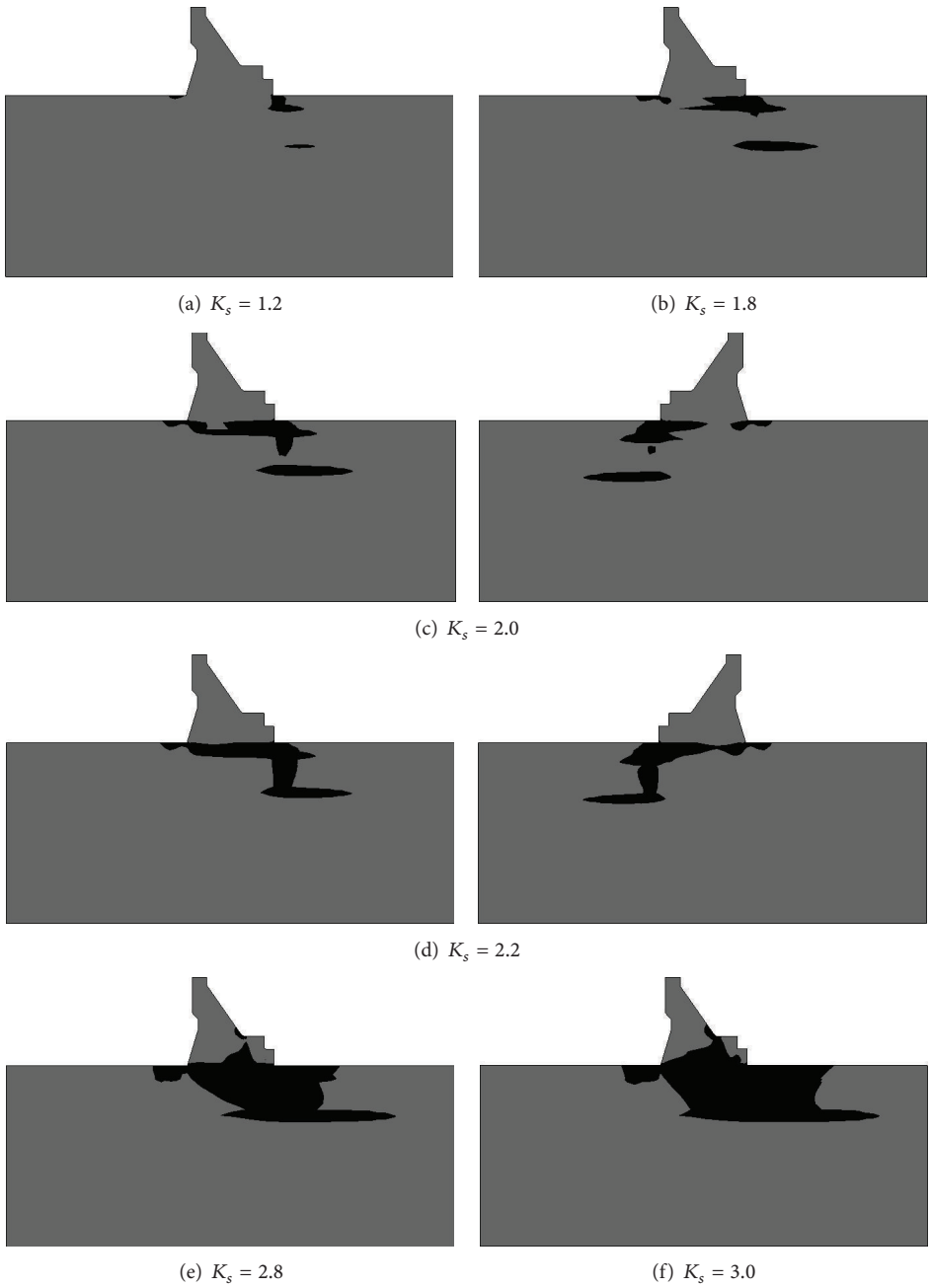

(a) $K_s = 1.2$ (b) $K_s = 1.8$

(c) $K_s = 2.0$

(d) $K_s = 2.2$

(e) $K_s = 2.8$ (f) $K_s = 3.0$

Figure 4: The progressive failure process of dam-foundation system under strength reduction.

along the weak interlayer is restricted by the downstream bedrocks. It seems that the totally connected yield zones between the foundation plane and the $t1_b$ interlayer from dam heel to dam toe will result in the rapid development of translational sliding of dam body and parts of the bedrocks after K_s reaches 2.2. However, the $t1_b$ interlayer is buried at an average depth of 30 m and horizontally distributed in the stream direction, so the development of the translational sliding is largely limited by the tail rock resistance blocks, and this phenomenon is better explained by one of the selected typical points which is on the foundation plane. When K_s exceeds 3.0, due to the existence of the downstream free surface of dam body, the connected yield zones in dam body result in the rapidly increased deformation at the upper of this dam. Therefore, catastrophes are shown on the displacement relation curves of the upper located typical points.

5.2.2. Analysis Results of the Overloading Method. Material strength of dam concretes and bedrocks are designed as the original values in the overloading method. Load condition is the same as that of the strength reduction method; the only difference is that the water density of upstream reservoir is increased to K_p times when the overloading parameter K_p is larger than 1.0; namely, only the upstream water pressure

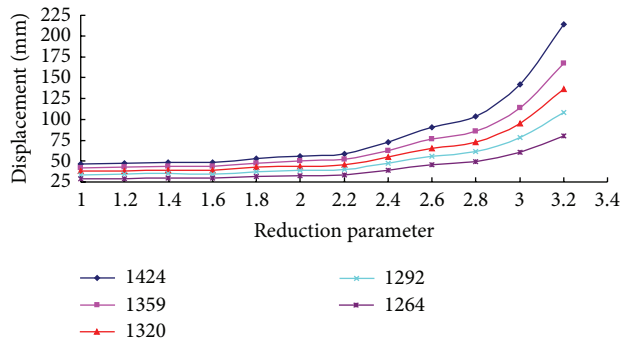

Figure 5: Relation curves between the stream displacement of dam body and the strength reduction parameter.

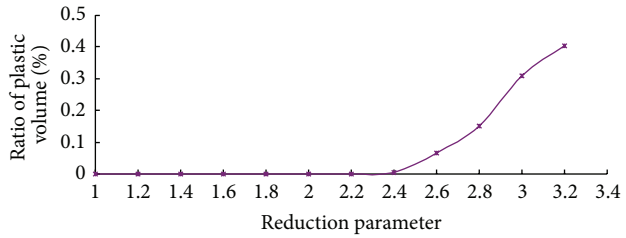

Figure 6: Relation curve between the yield volume ratio of dam body and the strength reduction parameter.

is increased when overloading. The overloading simulation process is that dam self-weight is firstly applied to model the pouring of dam concretes; then water pressure, silt pressure, and uplift pressure under the normal load condition are added, and the overloading is finally conducted by the continual increments of water density at an interval of 0.2 times.

The progressive failure process under the overloading method is shown in Figure 7, which is similar to the strength reduction method. As for the dam deformation of typical stages, such as the connectivity of plastic yield zones in bedrocks along the $t1_b$ interlayer from upstream to downstream, dam displacement by the overloading method is obviously larger than that of the strength reduction method at the same stage. When $K_p = 2.0$, the connectivity of yield zones completely appeared between the foundation plane and the $t1_b$ interlayer. Due to the existence of the folded slope of dam upstream surface, the total water weights on the upstream dam surface are also increased with the increments of upstream water density, which results in that the compression-shear yield zones are largely distributed in the bedrocks right below the dam heel. The strength of dam concretes is significantly higher than that of bedrocks; hence, except for some small parts of dam concretes close to the foundation plane, yield zones in dam body firstly appeared at the dam toe and the turning points of the upstream and downstream dam surface until K_p comes up to 2.8. With the continual increments of the overloading parameter, yield zones extend to the internal of dam body, and dam concretes at the turning point of the upstream dam surface yield rapidly. When $K_p = 3.6$, yield zones are connected in dam body from upstream to downstream.

Figure 8 shows the relation curves between the stream displacement of dam body and the overloading parameter. It can be seen that dam stream displacements of typical points at the elevation of 1424.0 m and 1359.0 m increase rapidly after K_p reaches 3.6. Reasons are that the connectivity of yield zones is formed in dam body when $K_p = 3.6$, and this yield zone works as a plastic hinge for the existence of the downstream dam free surface. Hence, the nonlinear deformation develops rapidly at the upper of the dam body.

It can be concluded from Figures 7 and 8 that the connectivity of yield zones already completely appeared between the foundation plane and the $t1_b$ interlayer when $K_p = 2.0$. However, displacement increasing rate of the five selected typical points is smaller until K_p reaches 3.0 (dam concretes begin to yield rapidly when $K_p = 3.0$). Therefore, for this concrete gravity dam, the connectivity of yield zones in dam foundation does not mean the loss of bearing capacity.

The relation curve between the yield volume ratio of dam body and the overloading parameter is shown in Figure 9. It can be seen that when $K_p = 2.4$, the yield volume ratio begins to increase with a smaller increasing rate. When $K_p = 3.0$, dam concretes yield rapidly, and the yield volume ratio has increased from 0.12 to 0.77 with the overloading parameter that ranges from 3.0 to 4.6. Water pressure on the top of the upstream dam surface increases slowly in the water density overloading method, so yield zones extend slowly to the dam crest after $K_p = 4.6$, and the yield volume ratio of dam body remains largely unchanged.

5.2.3. Analysis Results of the Comprehensive Method. To study the failure mechanism of instability under the comprehensive condition of abnormal environmental loads and material strength degradation or uncertainty, the comprehensive method has been conducted, and the simulation analysis results are concluded as follows.

Relation curves of stream displacement-overloading parameter at the foundation plane and dam crest are shown in Figures 10 and 11, respectively. The bigger strength reduction, the smaller overloading parameter is allowed when nonconvergence occurs, so these curves only reflect dam displacements before the overloading parameter K_p reaches 3.4. The development rule of displacement of the other three typical points are similar to this. Although for different strength reduction parameters, dam displacement changes stably and keeps almost the same values before K_p reaches 2.0. Therefore, under the comprehensive condition of abnormal environmental loads and a certain percentage of material strength degradation, displacement of this gravity dam will increase at a certain amplitude, while dam failure will not directly occur if the strength degradation and environmental loads are properly controlled.

Relation curves between the yield volume ratio of dam body and the overloading parameter under different strength reduction parameters are shown in Figure 12. It can be seen that strength reduction results in a reduced bearing capacity and the earlier occurrence of the catastrophe of concrete

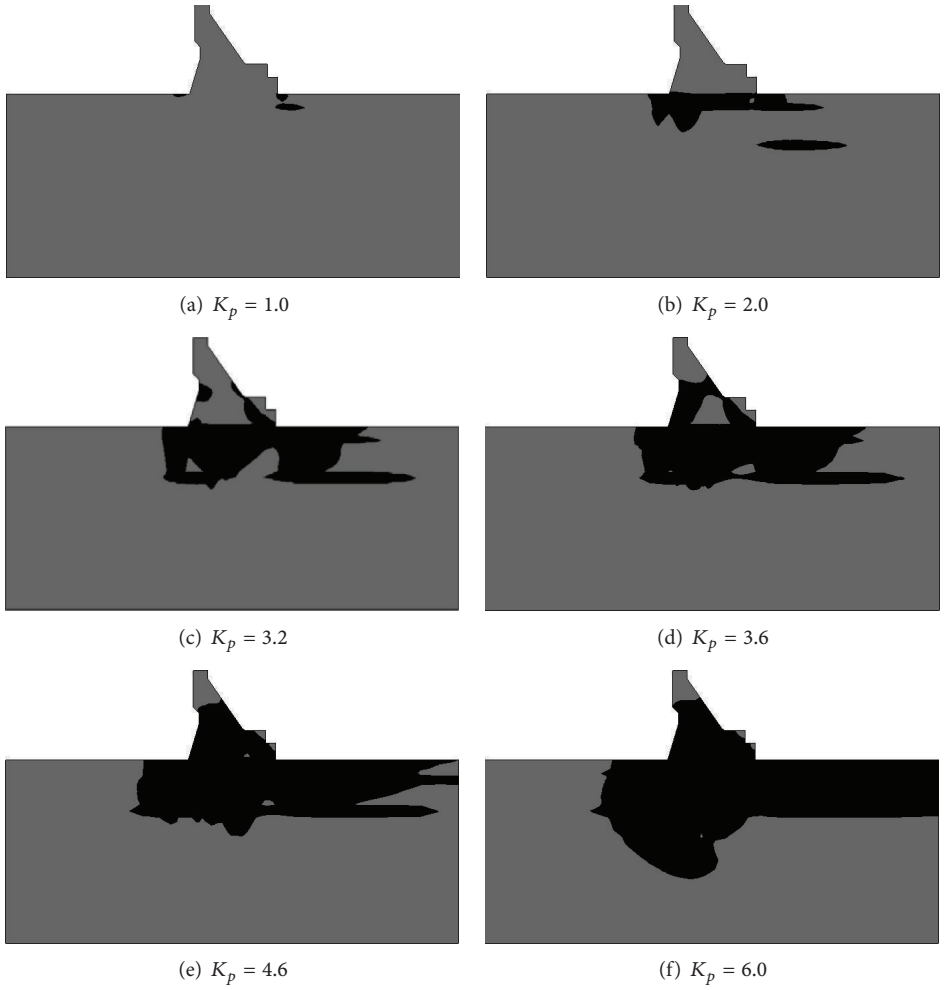

(a) $K_p = 1.0$ (b) $K_p = 2.0$

(c) $K_p = 3.2$ (d) $K_p = 3.6$

(e) $K_p = 4.6$ (f) $K_p = 6.0$

Figure 7: The progressive failure process of dam-foundation system under overloading.

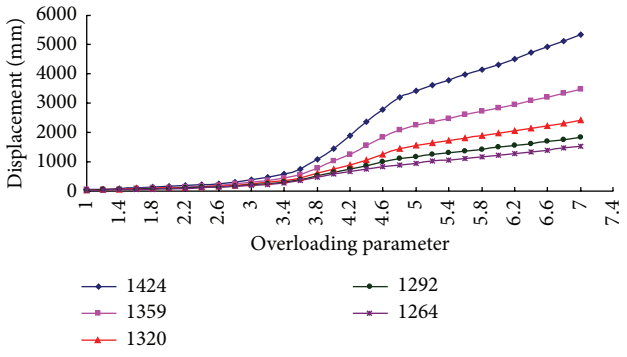

Figure 8: Relation curves between the stream displacement of dam body and the overloading parameter.

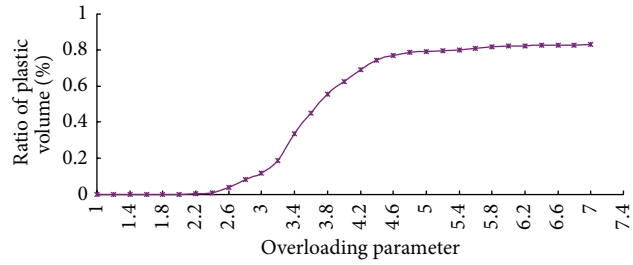

Figure 9: Relation curve between the yield volume ratio of dam body and the overloading parameter.

yield volume ratio. Dam overloading failures under different strength reduction conditions show that catastrophes of the yield volume ratio of dam concretes all appeared next to the connectivity of plastic yield zones between the foundation plane and the $t1_b$ interlayer and before the catastrophe of dam displacement. Therefore, catastrophe of the yield volume ratio of dam concretes does not mean the loss of bearing capacity for this concrete gravity dam, which should be determined according to whether the excessive plastic deformation will result in the catastrophe of dam displacement or not.

5.3. Instability Safety Monitoring Indexes. The progressive failure processes of this gravity dam section under the simulation methods of strength reduction and water density overloading are both represented as follows: plastic yield

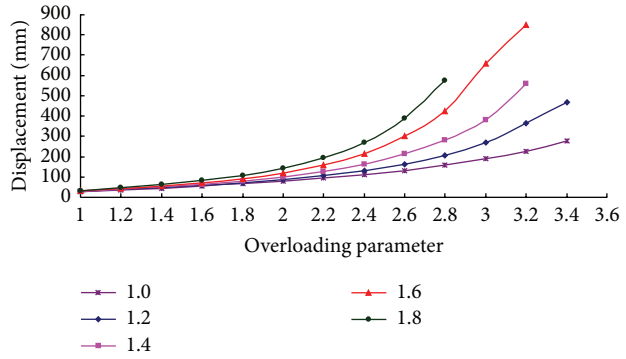

Figure 10: Relation curves between the stream displacement of the foundation plane and the overloading parameter under different strength reduction parameters.

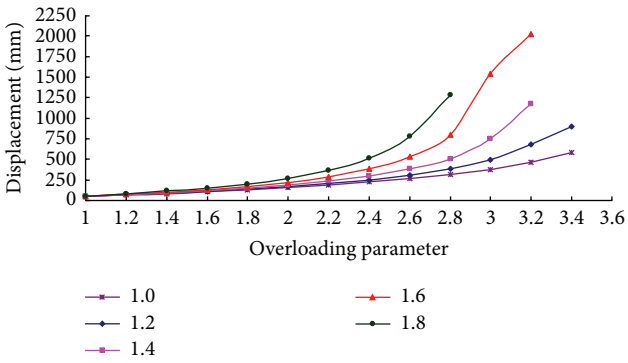

Figure 11: Relation curves between the stream displacement of the dam crest and the overloading parameter under different strength reduction parameters.

zones are firstly connected in bedrocks along the $t1_b$ weak interlayer; then, yield zones rapidly extend to dam body and result in the catastrophe of yield volume ratio of dam concretes; the rapidly increased excessive plastic deformation in dam body and foundation rocks results in the catastrophe of dam displacement, and the gravity dam loses the bearing capacity due to the failure of instability finally.

The aforementioned analyses show that catastrophes of the yield volume ratio of dam concretes in both simulation methods all appeared closely next to the connectivity of plastic yield zones between the foundation plane and the $t1_b$ interlayer. Therefore, there are two typical stages that can be defined in both failure processes: the first one is the connectivity of plastic yield zones along the $t1_b$ weak interlayer in bedrocks; the second one is the catastrophe of dam displacement.

During the designed service period, the potential most unfavorable conditions of dams are concluded as material strength degradation and extreme external environmental loads. Hence, methods of strength reduction and overloading can be, respectively, used in studying the failure mechanism of high concrete gravity dams under these two unfavorable conditions. Based on the dam safety monitoring system, dam theoretical displacements of typical points at

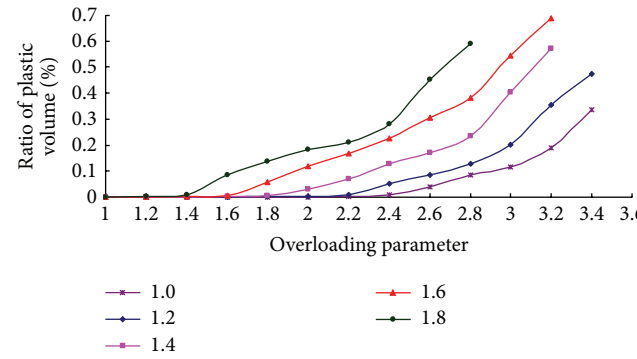

Figure 12: Relation curves between the yield volume ratio of dam body and the overloading parameter under different strength reduction parameters.

the aforementioned two typical stages can be determined as the safety monitoring indexes. Dam failure mechanism under the comprehensive method is similar to that of just overloading, and differences are only represented on the deformation that it is bigger for the same environmental loads when the material strength is reduced. Therefore, from the view of safety, the smaller displacement at the same typical stage is determined as the dam safety monitoring index; namely, monitoring indexes are hierarchically determined according to the theoretical results of strength reduction and overloading.

Research results of the strength reduction method show that the resisting force of the tail rock resistance block can be ensured due to the buried depth of 30 m and 80 m for $t1_b$ and $t1_a$, respectively. Therefore, although there are two weak interlayers distributed in bedrocks, the connectivity of plastic yield zones along the $t1_b$ interlayer will not result in the rapid development of the translational sliding. Dam displacements tend to be rapidly increased until dam concretes yield over large areas when K_s reaches 3.0. However, material property of dam concretes is easy to be identified and varies slightly for the better construction quality, so it is not inconsistent with the actual situation that the strength of all dam concretes can be determined as 1/3 of the original value due to the strength degradation or uncertainty. On the other hand, strength of bedrocks is usually weaker than that of dam concretes, and the strength degradation of bedrocks and weak structural surfaces are more serious than dam concretes for the obvious seepage in dam foundation. Theoretically speaking, dam failure of instability caused by material strength degradation or uncertainty will occur in dam foundation firstly. Therefore, based on the aforementioned analyses, catastrophe of dam displacement in the strength reduction method is not identified as the sign of losing bearing capacity for this concrete gravity dam.

Due to the complexity of rock genesis and geotectonic movement, various faults, joints, and cracks are complicatedly distributed in dam foundation, so big differences of material properties may appear in local small areas that cannot be systematically represented in geological survey. Therefore, under the normal condition, large deformation

Table 3: Monitoring indexes of dam stream displacement (unit: mm).

Elevation	Dam instability safety monitoring indexes		
	Grade one	Grade two	Grade three
1424 m	26.06	76.16	399.61
1359 m	18.89	44.86	213.60
1320 m	12.79	25.68	102.83
1292 m	7.00	12.43	45.26

which seems abnormal may also take place due to the uncertainty of rock properties, especially for the strength of weak structural surfaces, and dam safety will be threatened if and only if this uncertainty is beyond the range of acceptable. Therefore, the connectivity of yield zones along the $t1_b$ interlayer in the strength reduction method is defined as the variation sign of normal operation for this concrete gravity dam, and the corresponding dam displacement is determined as dam instability safety monitoring index of grade one. As for the connectivity of yield zones along the $t1_b$ interlayer caused by overloading, if engineering or nonengineering measures are not taken to stop the rapidly increased deformation (caused by the continual increments of environmental loads or the creep effect of bedrocks and dam concretes), it may result in the instability sliding of this gravity dam-foundation system. For the same typical stage of the connectivity of yield zones along the $t1_b$ interlayer, the risk level under overloading is more serious than that of strength degradation, so the second dam instability safety monitoring index is determined by the overloading method at the aforementioned dam failure stage.

Based on the aforementioned failure mechanism of instability, three grades of instability safety monitoring indexes are hierarchically determined for this high concrete gravity dam. The corresponding typical stages in the simulated dam failure process are identified as follows: (1) the first grade, the connectivity of plastic yield zones along the $t1_b$ interlayer from dam heel to dam toe by the strength reduction method with $K_s = 2.2$; (2) the second grade, the connectivity of plastic yield zones along the $t1_b$ interlayer from dam heel to dam toe by the overloading method with $K_p = 2.0$; (3) the third grade, catastrophe of dam displacement by the overloading method with $K_p = 3.6$. Monitoring indexes for the observation points of the plumb line are shown in Table 3. Here, the monitoring indexes of dam displacement are determined in terms of the foundation plane.

6. Conclusions

Aiming at the potential failure modes of material strength degradation and extreme external environmental loads during the service period, based on the FEM structural analysis method, failure mechanisms and the progressive failure process of high concrete gravity dams are studied in this paper by methods of strength reduction and overloading. Typical stages in the failure process are identified by evaluation indicators of dam displacement, the connectivity of yield zones, and the yield volume ratio of dam concretes; then instability safety monitoring index of high concrete gravity dams is determined according to these typical symptoms. At last, failure mechanism of a high concrete gravity dam is studied, and according to different dam safety situations, three grades of dam instability safety monitoring index of dam displacement are hierarchically established, which are, respectively, at the stages of the connectivity of yield zones along the weak interlayer by methods of strength reduction and overloading, and the catastrophe of dam displacement by the overloading method.

Acknowledgments

This work was supported by the Research Fund for the Doctoral Program of Higher Education of China (Grants nos. 20120094110005 and 20120094130003), the National Natural Science Foundation of China (Grants nos. 51379068, 51139001, 51279052, 51209077, and 51179066), the Program for New Century Excellent Talents in University (Grant no. NCET-11-0628), and the Ministry of Water Resources Public Welfare Industry Research Special Fund Project (Grants nos. 201201038 and 201101013).

References

[1] C. S. Gu, B. Li, G. L. Xu, and H. Yu, "Back analysis of mechanical parameters of roller compacted concrete dam," *Science China Technological Sciences*, vol. 53, no. 3, pp. 848–853, 2010.

[2] H. Yu, Z. R. Wu, T. F. Bao, and L. Zhang, "Multivariate analysis in dam monitoring data with PCA," *Science China Technological Sciences*, vol. 53, no. 4, pp. 1088–1097, 2010.

[3] Y. Q. Ni, X. W. Ye, and J. M. Ko, "Monitoring-based fatigue reliability assessment of steel bridges: analytical model and application," *Journal of Structural Engineering*, vol. 136, no. 12, pp. 1563–1573, 2010.

[4] X. W. Ye, Y. Q. Ni, K. Y. Wong, and J. M. Ko, "Statistical analysis of stress spectra for fatigue life assessment of steel bridges with structural health monitoring data," *Engineering Structures*, vol. 45, pp. 166–176, 2012.

[5] X. W. Ye, Y. Q. Ni, and Y. X. Xia, "Distributed strain sensor networks for in-construction monitoring and safety evaluation of high-rise building," *International Journal of Distributed Sensor Networks*, vol. 2012, Article ID 685054, 13 pages, 2012.

[6] C. S. Gu, E. F. Zhao, Y. Jin, and H. Z. Su, "Singular value diagnosis in dam safety monitoring effect values," *Science China Technological Sciences*, vol. 54, no. 5, pp. 1169–1176, 2011.

[7] L. Chen, *Mechanics Performance With Parameters Changing in Space and Monitoring Models of Roller Compacted Concrete Dam*, College of Water Conservancy and Hydropower Engineering, Hohai University, Nanjing, China, 2006 (Chinese).

[8] P. Lei, *Study on the Theory and Method of Deformation Monitoring Index of Concrete Dam*, College of Water Conservancy and Hydropower Engineering, Hohai University, Nanjing, China, 2008 (Chinese).

[9] H. Z. Su, J. Hu, J. Y. Li, and Z. R. Wu, "Deep stability evaluation of high-gravity dam under combining action of powerhouse and dam," *International Journal of Geomechanics*, vol. 13, no. 3, pp. 257–272, 2013.

[10] H. Z. Su, J. Hu, and Z. P. Wen, "Service life predicting of dam systems with correlated failure modes," *Journal of Performance of Constructed Facilities*, vol. 27, no. 3, pp. 252–269, 2013.

[11] S. L. Fan, J. Y. Chen, and J. Y. Guo, "Application of finite element equivalent stress method to analyze the strength of gravity dam," *Journal of Hydraulic Engineering*, vol. 38, no. 6, pp. 754–766, 2007 (Chinese).

[12] H. Z. Su, Z. R. Wu, Y. C. Gu, J. Hu, and Z. P. Wen, "Game model of safety monitoring for arch dam deformation," *Science in China E*, vol. 51, no. 2, pp. 76–81, 2008.

[13] C. S. Gu and Z. R. Wu, *Safety Monitoring of Dams and Dam Foundations-Theories & Methods and Their Application*, Hohai University Press, Nanjing, China, 2006 (Chinese).

[14] Z. Z. Shen, M. Ma, and X. X. Tu, "Early warning index of deformation for gravity dam based on discontinuous deformation analysis," *Journal of Hydraulic Engineering*, vol. 38, supplement, pp. 94–99, 2007 (Chinese).

[15] D. J. Zheng, Z. Y. Huo, and B. Li, "Arch-dam crack deformation monitoring hybrid model based on XFEM," *Science China Technological Sciences*, vol. 54, no. 10, pp. 2611–2617, 2011.

[16] P. Lei, X. L. Chang, F. Xiao, G. J. Zhang, and H. Z. Su, "Study on early warning index of spatial deformation for high concrete dam," *Science China Technological Sciences*, vol. 54, no. 6, pp. 1607–1614, 2011.

[17] Y. C. Gu and S. J. Wang, "Study on the early-warning threshold of structural instability unexpected accidents of reservoir dam," *Journal of Hydraulic Engineering*, vol. 40, no. 12, pp. 1467–1472, 2009 (Chinese).

[18] C. S. Shen, S. X. Wang, Y. C. Lin, and X. Q. Liu, *Hydraulic Structure*, China Water Power Press, Beijing, China, 2008 (Chinese).

[19] X. L. Chang, H. Wang, W. Zhou, and C. B. Zhou, "Mechanism of two sliding failure modes in gravity dam and method for safety evaluation," *Journal of Hydraulic Engineering*, vol. 40, no. 10, pp. 1189–1195, 2009 (Chinese).

[20] F. Jin, W. Hu, J. W. Pan, J. Yang, J. T. Wang, and C. H. Zhang, "Failure analysis of high-concrete gravity dam based on strength reserve factor method," *Computers and Geotechnics*, vol. 35, no. 4, pp. 627–636, 2008.

[21] F. Jin, W. Hu, J. W. Pan, J. Yang, J. T. Wang, and C. H. Zhang, "Comparative study procedure for the safety evaluation of high arch dams," *Computers and Geotechnics*, vol. 38, no. 3, pp. 306–317, 2011.

[22] G. X. Zhang, Y. Liu, and Q. J. Zhou, "Study on real working performance and overload safety factor of high arch dam," *Science in China E*, vol. 51, no. 2, pp. 48–59, 2008.

[23] D. J. Zheng and T. Lei, "Instability criteria for high arch dams using catastrophe theory," *Chinese Journal of Geotechnical Engineering*, vol. 33, no. 1, pp. 23–27, 2011 (Chinese).

[24] State Economic and Trade Commission of China [SETCC]. Specifications for seismic design of hydraulic structures DL5073-2000, 2001 (in Chinese).

[25] MSC, *Software Corporation. MSC. Marc Vol. A: Theory and User Information*, MSCSoftware Corporation, Santa Ana, Calif, USA, 2005.

[26] Y. R. Zheng, S. Y. Zhao, W. X. Kong, and C. J. Deng, "Geotechnical engineering limit analysis using finite element method," *Rock and Soil Mechanics*, vol. 26, no. 1, pp. 163–168, 2005 (Chinese).